T15A
0159

Acoustic constraints on semi-brittle deformation of Carrara marble

Hilary Chang*, H O. Ghaffari, Ulrich Mok, J Brian Evans and Matej Pec
*Contact: hilarych@mit.edu
Massachusetts Institute of Technology

Semi-brittle deformation

- **The semi-brittle regime** is a transition between brittle to ductile deformation, where rocks fail with increasing degree of plasticity under increasing pressure, temperature, or decreasing strain rate.

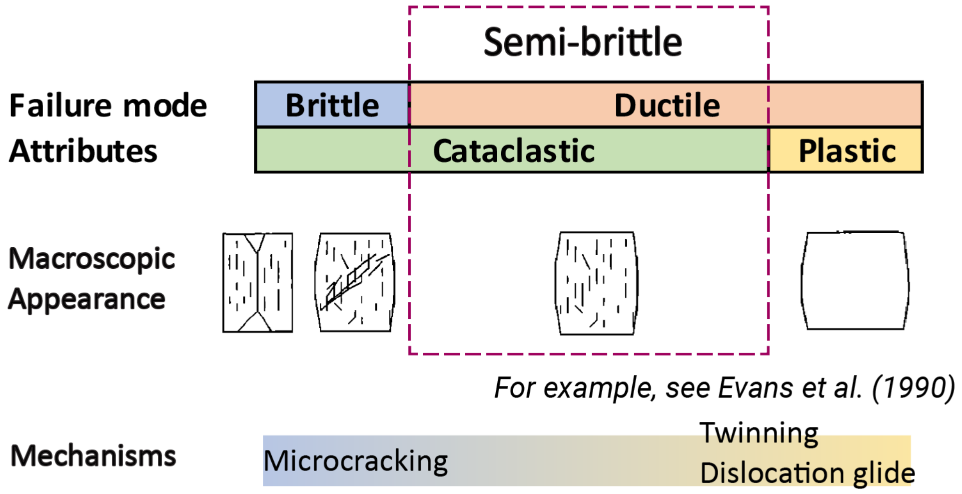

For example, see Evans et al. (1990)

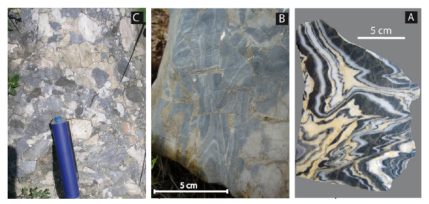

From brittle to fully plastic deformation in mylonitic marble. Lagabrielle et al. (2016)

Simulating condition at the brittle-ductile transition: Experiment setup

- To investigate the mechanisms involved during semi-brittle flow, we deform **Carrara marble** over a **confining pressure (Pc)** range of **0.1-300 MPa** at room temperature.
  - Apply triaxial load to intact, dry rock sample.
  - Under constant strain rate (~10^{-4} s^{-1}) to a final strain of ~10%.
  - Collect data: Axial displacement, applied load, active ultrasound pulsing, acoustic emissions (AEs).

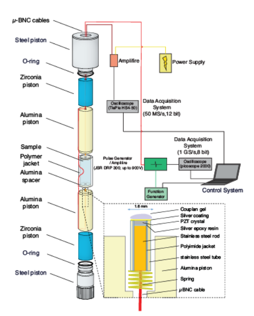

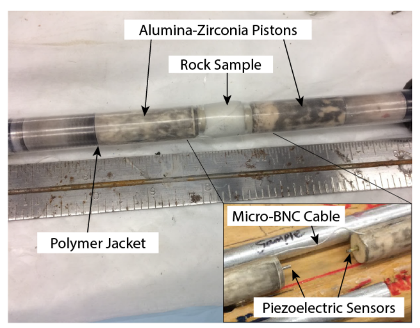

The Paterson gas medium apparatus can routinely reach Pc up to 300 MPa. We modified it to collect passive and active ultrasound data.

Elastic velocity evolution

- We use active ultrasound pulsing to estimate the P wave velocity (Vp).
- The waveform correlation-based method allows us to track precise travel time changes.

Vp increases logarithmically with increasing Pc.

$V_p = 126.36\ln(5.16P_c) + 5519$ m/s

Consistent with Burlini & Kunze (2000).

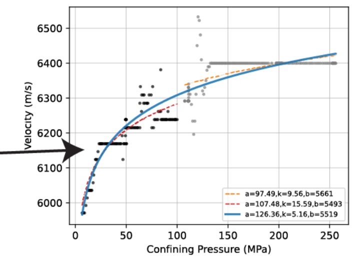

- During the deformation stage:

Vp increases initially before yielding.

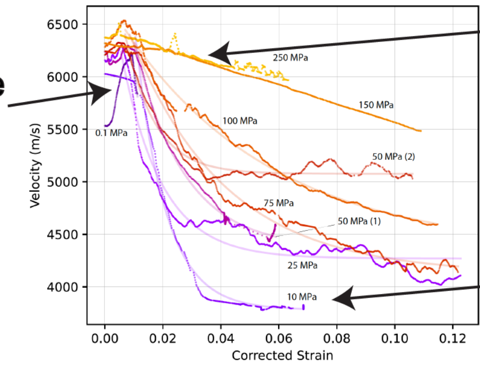

Vp decays drastically after yielding.

More drastic decay at lower Pc.

- Prevalent crackings after yielding at low Pc causes larger velocity decay (Guéguen & Schubnel, 2003).
  Consistent with Schubnel et al., (2005), Schubnel et al., (2006).

Mechanical response and microstructure

- Mechanical observations agree with previous studies for intact Carrara marble (Fredrich et al. 1989; for rock with existing fault, see Meyer et al., 2019).

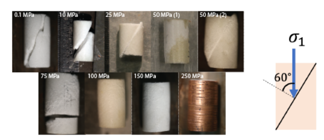

A major fault developed at Pc ≤ 50 MPa. Sample length ~ 2 cm.

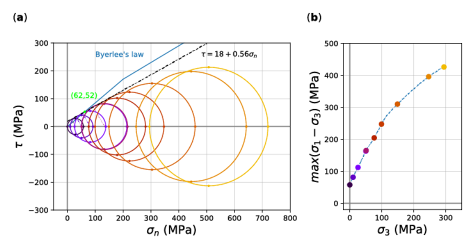

Mohr-Coulomb (M-C) envelope deviating from linear at Pc > 200 MPa suggests ductile deformation. Pc=64 MPa corresponds to the intersection of M-C envelope with Byerlee's law and the disapearance of macroscopic fault.

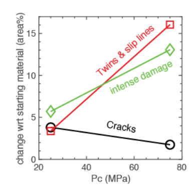

Increasing activity of crystal-plastic deformation machanism with increasing confining pressure (Pc).

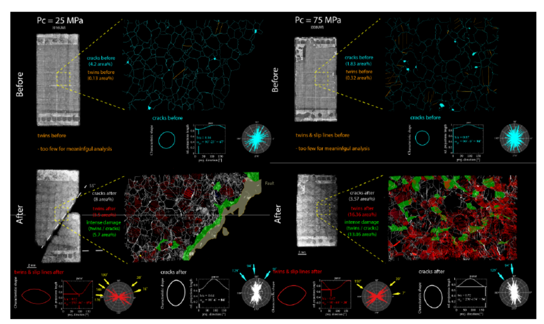

Acoustic emissions (AEs)

AE rate decreases at yield point.

AE rate decreases when Pc>~50 MPa. (with the exception of the experiment at 100 MPa)

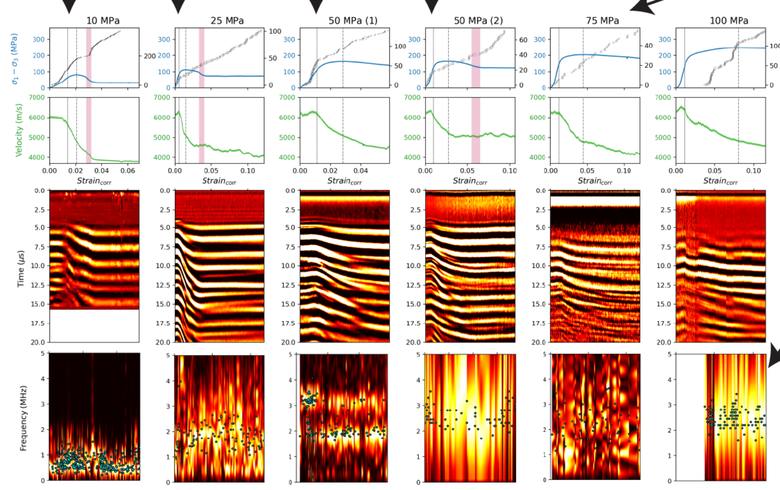

AE's shift
- **to higher frequencies at higher Pc.**
- **to lower frequencies at larger strain.**

*Comparison of the deformation stages of 6 experiments from Pc=10-100 MPa (left to right). [1st row] Stress-strain curve (blue), AEs (black circles), **yield point and peak stress (the 1st and 2nd dashed lines)**, failure (red shade); [2nd row] Vp (green); [3rd row] Pulsing waveform (t=0 is source time); [4st row] AE spectra, median frequencies (cyan dots).*

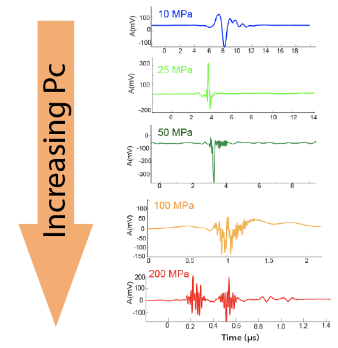

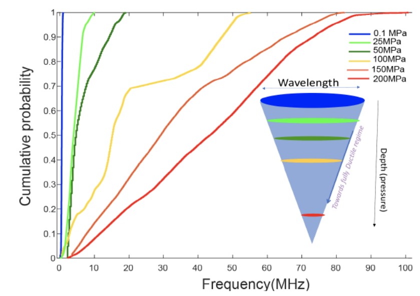

AE waveforms at higher Pc show higher frequency contents.

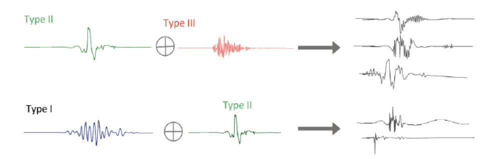

The waveforms can be decomposed into three types of waveforms, likely related to different mechanisms.

- **During semi-brittle deformation, the elastic velocity increases before yielding and decreases drastically afterward due to damage. At higher Pc, the slower decay of velocity with increasing strain is related to increasing crystal-plastic deformation for strain accomodation.**
- **We record high-frequency ultrasound acoustic emissions (AEs) for the first time. These high-frequency AEs are more abundant at higher confining pressures (Pc) and are potentially associated with plastic mechanisms such as twinning and dislocation avalanches.**

References:

Burlini, L., & Kunze, K. (2000). Fabric and seismic properties of Carrara marble mylonite. Physics and Chemistry of the Earth, Part A: Solid Earth and Geodesy, 25(2), 133-139
Evans, B., Fredrich, J. T., & Wong, T. F. (1990). The brittle-ductile transition in rocks: Recent experimental and theoretical progress. The Brittle-Ductile Transition in Rocks, Geophys. Monogr. Ser, 56, 1-20.
Fredrich, J. T., Evans, B., & Wong, T. F. (1989). Micromechanics of the brittle to plastic transition in Carrara marble. Journal of Geophysical Research: Solid Earth, 94(B4), 4129-4145.
Guéguen, Y., & Schubnel, A. (2003). Elastic wave velocities and permeability of cracked rocks. Tectonophysics, 370(1-4), 163-176.
Lagabrielle, Y., Clerc, C., Vauchez, A., Lahfid, A., Labaume, P., Azambre, B., ... & Dautria, J. M. (2016). Very high geothermal gradient during mantle exhumation recorded in mylonitic marbles and carbonate breccias from a Mesozoic Pyrenean palaeomargin (Lherz area, North Pyrenean Zone, France). Comptes Rendus Géoscience, 348(3-4), 290-300.
Meyer, G. G., Brantut, N., Mitchell, T. M., & Meredith, P. G. (2019). Fault reactivation and strain partitioning across the brittle-ductile transition. Geology, 47(12), 1127-1130.
Schubnel, A., J. Fortin, L. Burlini, and Y. Gueguen (2005), Damage and recovery of calcite rocks deformed in the cataclastic regime, in High-Strain Zones: Structure and Physical Properties. Special Publication 245, edited by D. Bruhn and L. Burlini, pp. 203-221, Geological Society, London.
Schubnel, A., Walker, E., Thompson, B. D., Fortin, J., Guéguen, Y., & Young, R. P. (2006). Transient creep, aseismic damage and slow failure in Carrara marble deformed across the brittle-ductile transition. Geophysical Research Letters, 33(17).